Journal of Materials Chemistry

Dynamic Article Links

Cite this: *J. Mater. Chem.*, 2012, **22**, 12718

www.rsc.org/materials

PAPER

Single-component room-temperature discotic nematic liquid crystals formed by introducing an attraction-enhancing in-plane protrusion onto the hexa(phenylethynyl)benzene core†

Hsiu-Hui Chen, Hsin-An Lin, Shih-Chieh Chien, Tsai-Hui Wang, Hsiu-Fu Hsu,* Tzenge-Lien Shih* and Chunhung Wu

Received 30th November 2011, Accepted 30th April 2012
DOI: 10.1039/c2jm16263f

Single-component room-temperature discotic nematics have been achieved within large temperature ranges by introducing an attraction-enhancing protrusion onto hexa(phenylethynyl)benzenes. X-ray diffraction investigations revealed the nematic phases of these new discotic nematic materials to be cybotactic.

Introduction

Disc-like molecules with nematic superstructures have attracted great interest recently in view of demands for materials utilized in fabricating compensating films[1,2] or for potential materials as active liquid crystals (LCs), both for improving viewing angle characteristics of liquid crystal displays (LCDs). In addition to the application in LCDs, discotic nematics also found applications as lubricants in a tiny space.[3,4] Relative to a mass number of calamitic nematogens, only a few disc-like molecules were reported to show the discotic nematic (N_D) phase.[5–12] Often, disc-like molecules are prone to packing into columnar superstructures due to strong inter-disc interactions, *e.g.* π–π interactions between the usually planar large core structures. However, for multiynylbenzenes,[7,8,10,12] one of the most investigated discotic nematogens, the rotational freedom of the side-arms prevents efficient disc stacking for column formation and reduces inter-disc attractions to slide discs off columns to form nematic superstructures. Unfortunately, N_D phases are usually observed with narrow mesophase ranges and high transition temperatures, especially high melting points (T_ms). In view of the aforementioned practical applications, room-temperature discotic nematics are highly in demand. Recently, two systems have been reported to achieve room-temperature discotic nematics, one by eutectic mixtures of hexaynylbenzenes[13,14] and one by a triphenylene derivative complexed with ions.[15] Both examples used mixtures to accomplish room-temperature melting points. A general strategy that leads to single-component room-temperature N_D materials with reasonable ranges has yet been disclosed.

To obtain the discotic nematic packing motif, a delicate balance of complex intermolecular interactions is crucial, otherwise, columnar supra-structures form or no LC behaviour occurs. As for the well known discotic nematogenic multiynylbenzenes, the molecular packing of hexakis(4-hexyloxyphenylethynyl)benzene (**1**),[16] in the crystal structure provides information on inter-disc interactions in the solid state. Along disc normal, one peripheral phenyl ring in one disc shows offset face-to-face π–π interactions with two peripheral phenyl rings from adjacent two discs, one above and one below. Along the molecular plane, chain inter-digitation is responsible for inter-discotic interaction. When melting, these attractions are expected to be lessened by the aforementioned side-arm rotational freedom to lead to a N_D phase. Replacing all the peripheral phenyl rings in hexakis(pentylphenylethynyl)benzene (**2a**, N_D between 170 and 185 °C)[12] with six biphenyls led to a significantly extended liquid crystal range (**3**, columnar between 170 and 240 °C) with the same melting point at the expense of losing the discotic nematic phase to form a columnar mesophase.[10] The six-fold enhancement of attractions by biphenyls was excessive to retain the nematic arrangement and hence induced the formation of a columnar phase. Recently, we reported a new concept of introducing lateral substitutions to one side-arm of modification of nematogenic hexaynylbenzenes for achieving N_D materials with significantly low melting points and wide mesophase ranges.[17] Yet, room-temperature N_D materials could not be achieved. Herein, these two designs, single sidearm modification of nematogenic hexaynylbenzenes[18–20] and installation of the attraction-enhancing biphenyl unit, are combined to afford wide-range room-temperature N_D materials (Scheme 1).

Results and discussion

Compound **1** (ref. 7 and 17) was chosen over its alkyl analogue **2** (ref. 12) as the starting model compound to be further derivatized

Department of Chemistry, Tamkang University, Tamsui 251, Taiwan. E-mail: hhsu@mail.tku.edu.tw; Fax: +886-2-2620-9924

† Electronic supplementary information (ESI) available: General procedure, additional optical textures and thermogravimetric (TGA) analysis data. See DOI: 10.1039/c2jm16263f

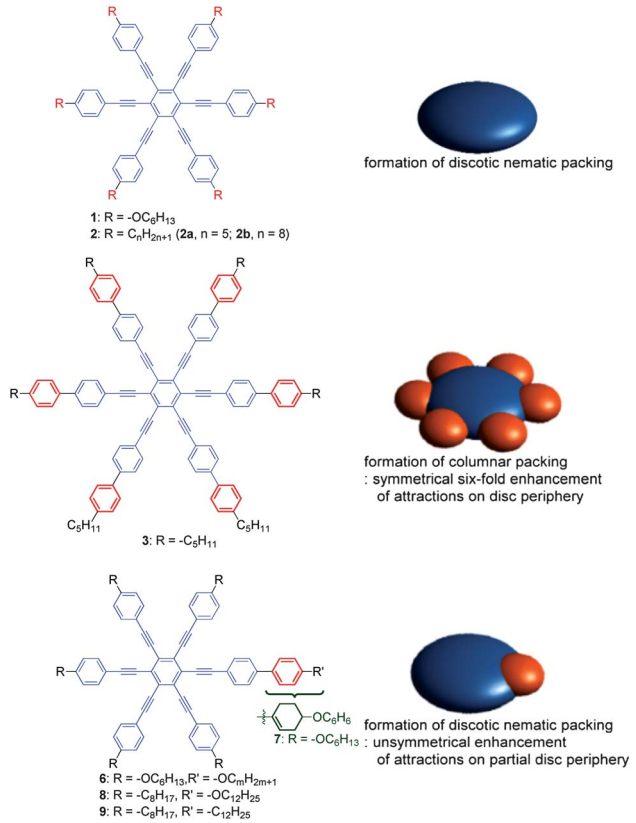

Scheme 1 Left: chemical structures of compounds **1–3** and **6–9**. Right: schematic representations of respective cores of the structures are shown at the left except **7** (red: attraction-enhancing extrusion units).

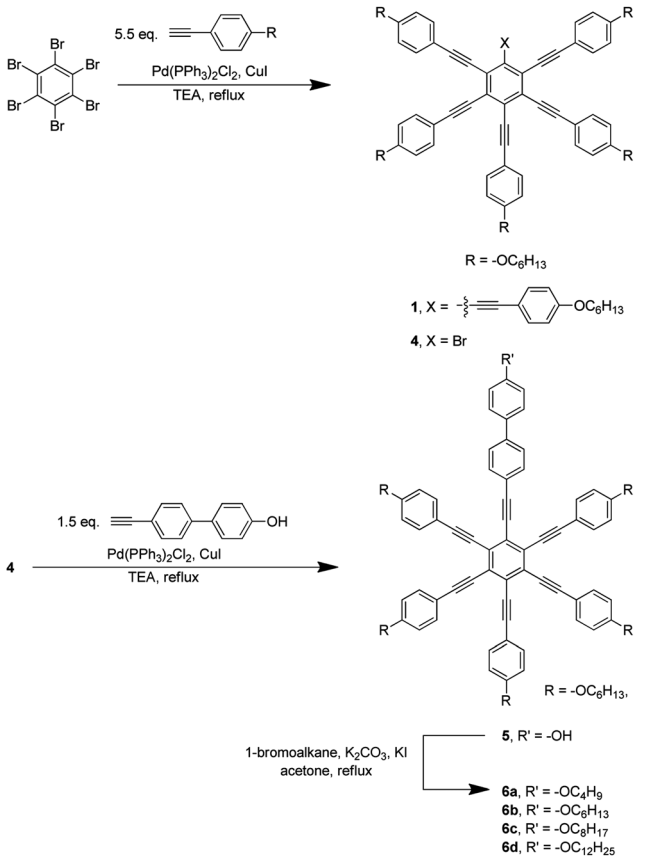

Scheme 2 Synthetic scheme for compounds **1**, **4**, **5**, and **6**.

due to its wider N_D range. The synthesis of **6** is shown in Scheme 2. By reacting 5.5 equivalents of the 1-ethynyl-4-hexyloxybenzene with hexabromobenzene under Sonogashira coupling conditions, the pentaynylbromobenzene (**4**) was obtained in optimized 36% yield. Also produced were the hexaynylbenzene derivative (**1**) and compounds of other incomplete substitutions. Further coupling of 4′-ethynyl-biphenyl-4-ol with **4** afforded 4′-[pentakis(4-hexyloxyphenylethynyl)phenylethynyl]biphenyl-4-ol (**5**) in 79% yield. Alkylation of the hydroxyl group on the biphenyl gave series **6** compounds in quantitative yields.

The mesomorphic properties of **6a–6d** studied by polarizing optical microscopy (POM) and differential scanning calorimetry (DSC) are summarized in Table 1. All series **6** compounds exhibit a N_D phase, identified by their characteristic Schlieren textures (Fig. S1 in ESI†). The replacement of one peripheral phenyl in **1** (N_D: between 144 and 216 °C) with a biphenyl unit does not induce the formation of columnar phases.[17] Moreover, compound **6b** shows a 36-degree decrease in T_m and a 13-degree increase in clearing temperature (T_c) to give an expansion of 49 degrees in the nematic range. The lower melting point of **6b** is attributed to the resulting lower packing efficiency by both the lower molecular symmetry and the non-ideal disc-like molecular core with a protruding phenyl. The wider mesophase range is ascribed to the stronger inter-disc attractive interactions provided by the introduced biphenyl unit. Varying the chain length of the unique biphenyl-containing side-arm gave further movement of the transition temperatures. Both the melting and clearing points decrease with increasing chain length of the unique sidearm. Among **6a–6d**, **6d** shows the widest mesophase range and the lowest melting point of 70 °C, 74 degrees lower than that of **1**. Moreover, **6d** is the only one with no signs of decomposition prior clearing. All series **6** compounds showed a decomposition temperature (5% decomposition) above 300 °C; however, minor decomposition can be detected at *ca.* 200 °C (Fig. S2 and S3 in ESI†).

To examine the function of the bulged phenyl, a cyclohexnyl unit was used to replace the protruded phenyl in **6b** to afford compound **7**. The N_D phase of **7** is observed between 81 and

Table 1 Mesogenic behaviours[a] of compounds **6a–6d** and **7–9**

	K	T_m	N_D	T_c	I	Range
6a	●	125.2	●	235.0	●[b]	110
6b	●	107.8	●	228.6	●[b]	121
6c	●	83.2	●	200.0[b]	●[b]	117
6d	●	70.0	●	198.7	●	129
7	●	81.4	●	152.0	●	71
8	●	39.8	●	108.8	●	69 (1st run)
	●	18.0	●	112.2	●	94 (2nd run)
9[c]	●	11.4	●	55.9	●	45

[a] T_m and T_c: melting and clearing temperatures in °C of the 2nd heating run from DSC. [b] Partial decomposition upon clearing under POM. [c] Data from 1st and 2nd runs are the same.

152 °C. In addition to the T_m lowering by the protrusion from the disc in **6b** from the circular core geometry of **1**, the bulkiness of the cyclohexenyl ring in **7** has imposed a further significant T_m reduction of 26 degrees. However, a more pronounced T_{NI} lowering of 77 degrees also results from the structural modification in **7** from **6b** to give a significant shrinkage of 50 degrees in the N_D range. The lowering on both T_m and T_{NI} is ascribed to the bulkier cyclohexnyl moiety for less efficient packing. These results demonstrate that a protrusion from a nematogenic discotic hexaynyl core can lead to a significant melting temperature descending; however, an attraction-enhancing protrusion is necessary for maintaining or even improving the N_D range.

As aforementioned, hexakis(4-alkylphenylethynyl)benzenes (**2**)[12] were known to exhibit considerably lower melting points than their corresponding alkoxy analogues (**1**),[7,17] among which the octyl derivative (**2b**) showed the lowest T_m of 80 °C. By replacing one sidearm in **2b** with a 4-(dodecyloxy)-4′-ethynyl-1,1′-biphenyl, compound **8** (Scheme 1) was synthesized. Excitingly, compound **8** shows the typical N_D Schlieren texture between 18 and 112 °C in the second heating run. However, the nematic phase of **8** in the first heating run was found to be between 40 and 109 °C. Such varied phase behaviour with the thermal history is very different from that of **6d**, which exhibited similar thermal behaviours in all thermal treatment runs. Comparing to **6d**, compound **8** exhibits a T_m being 52 degree lower to be below room temperature without sacrificing too much on the nematic range. With a rational design, a single-component room-temperature discotic nematic material with a large temperature range is achieved. Compared with the thermal behaviour of the model compound **2b** (N_D: 80–96 °C), compound **8** shows not only a noteworthy 62-degree drop of the melting point but also a 16-degree rise in the clearing point to give a large expansion of 78 degrees of the nematic range.

As aforementioned, though compound **8** exhibits a discotic nematic phase at room temperature, its phase behaviour is varies significantly with the thermal history. Compound **9** was designed and prepared in hope to lead to a material with a room-temperature N_D phase in all thermal treatment runs. Compound **9** does achieve a sub-room-temperature T_m in first and second heating runs to show a N_D phase between 11 and 56 °C. Under POM, homeotropic textures are observed for **9** sandwiched between glass slides. However, Schlieren textures can be obtained as shown in Fig. 1(a) when the cover slide was removed. The nematic range was significantly expanded to 45 degrees for **9** comparing to 16 degrees for **2b**. On the other hand, when compared to the 94-degree nematic range of **8**, the nematic range of **9** is shrunk to approximately an half, which signifies the important role of the ether linkage for attaining a wide nematic range.

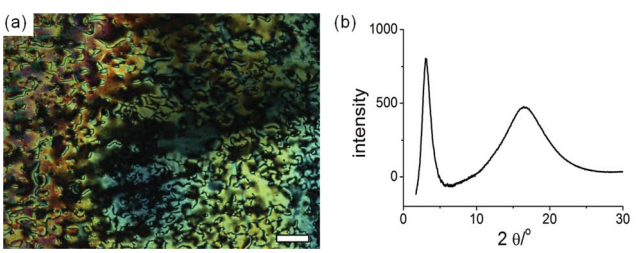

Fig. 1 (a) Micrographs of 8 at 25 °C (scale bar: 50 mm) and (b) X-ray diffractogram of compound **9** in the nematic phase on cooling at 25 °C.

Compounds **6b**, **6d**, **7**, **8**, and **9** were further investigated by powder X-ray diffraction (XRD) investigations for the realization of inter-disc interactions on the their thermal properties and the results are tabulated in Table 2. XRD data of compounds **1** and **2b** are also listed for comparison.[17] The diffractograms of the nematic phases of **9** in the nematic phase at RT are shown in Fig. 1(b). Within the respective nematic temperature range, all biphenyl derivatives, compounds **6b**, **6d**, **8**, and **9**, showed the typical nematic diffraction pattern, one broad reflection in the small angle regime and one even broader halo in the wide angle area. The small angle signal represents the average inter-disc distance along the disc plane, and the large angle halo is mainly originated from the liquid-like correlation of the molten chains though the average inter-disc distance along the disc normal may also locate in the same regime. With an additional *n*-hexyl unit in **6d**, only an increase of 3 Å in inter-disc distance is found, indicating that the contribution of the increased chain length in the unique sidearm on inter-disc separation has been averaged out.

The influence of the incorporated biphenyl moiety on the nematic supra-structure can be realized by cluster-size analysis on the diffractograms. For compounds **6b**, **6d**, **8**, and **9**, the longitudinal and transversal cluster sizes, $L_{\parallel}$ and $L_{\perp}$, by Scherrer's equation, within the nematic temperature range are listed in Table 2. Compared to compound **1**, compounds **6a** and **6b** exhibit slightly larger cluster sizes along disc plane and similar cluster sizes along disc normal. Similar effects are also found when comparing compounds **8** and **9** with **2b**. The calculated cluster sizes, $L_{\parallel}$ and $L_{\perp}$, of these compounds in the nematic phase correspond to an aggregate of *ca.* three ($L/d + 1$) molecules both in longitudinal and transversal directions to lead to the nematic phase by these compounds to be the cybotactic[21,22] discotic nematic phase, denoted as $N_{D\text{-}cyb}$, which was also supported by the relatively higher intensity of the small-angle signal with respect to that of the wide angle signal. The wider nematic range of compounds **6a**, **6b**, **8**, and **9** than the corresponding model compounds **1** and **2** may be ascribed to their larger cluster sizes than those of model compounds. Moreover, the slightly enhanced $L_{\parallel}$s and the unchanged $L_{\perp}$s of the studied compounds are not large enough to induce columnar formation.

Table 2 X-ray reflections and cluster sizes (L) of the nematic phases in **1**,[17] **6b**, **6d**, **2b**,[8] **8**, and **9**

		d (Å)					
	T (°C)	SAXS	WAXS	$L_{\parallel}$ (Å)	$L_{\parallel}/d$	$L\perp$ (Å)	$L\perp/d$
1	185	21.2		38.4	1.8		
			4.6			7.2	1.6
6b	160	20.2		40.0	2.0		
			4.4			7.1	1.6
6d	180	23.2		47.1	2.0		
			4.8			7.2	1.5
2b	100	22.1		40.8	1.8		
			4.4			8.6	1.9
8	100	23.2		47.1	2.0		
			4.6			9.2	2.0
9	70	24.3		56.3	2.3		
			4.6			9.0	2.0

Conclusions

In conclusion, incorporation of a protrusion onto a discotic nematogen is found to effectively lower melting points by the lower molecular symmetry and the non-ideal-disc core, both resulting in inefficient molecular packing. When the protrusion moiety is attraction-enhancing, the nematic temperature range can be expanded without the induction of columnar phases. The combination of attraction-enhancing protrusion from disc and incorporation of alkyl chains rather than alkoxy ones have been practised on nematogenic hexaynylbenzenes to provide single-component room-temperature discotic nematic materials. Applications of the strategy onto other N_D systems are worth investigating for developing more room-temperature discotic nematics as materials for manufacturing wide view angle films for LCDs.

Experimental

4,4′,4″,4‴,4⁗-((6-Bromobenzene-1,2,3,4,5-pentayl)-pentakis(ethyne-2,1-diyl))pentakis((hexyloxy)benzene) (5)

4′-Ethynyl-1,1′-biphenyl-4-ol (2.40 mg, 3.88 mmol) in triethylamine (20 mL) was added dropwise to a mixture of trans-dichlorobis(triphenylphosphine)palladium(II) (0.21 g, 0.26 mmol), copper iodide (0.10 g, 0.52 mmol), triphenylphosphine (0.15 g, 0.52 mmol), 1-bromo-2,3,4,5,6-pentakis(4-hexyloxyphenylethynyl)benzene (3.00 g, 2.59 mmol) and triethylamine (20 mL) under an nitrogen atmosphere at reflux. The mixture was stirred at reflux for 4 h. After cooling, to the reaction mixture was added dichloromethane (100 mL). The mixture was washed with NH_4Cl(aq) (100 mL × 2), H_2O (100 mL × 2), and dried over $MgSO_4$. After removal of the solvents, the residue was purified by column chromatography (SiO_2, *n*-hexane–dichloromethane 2 : 1) and crystallized from *n*-hexane to yield **5** as a yellow powder (2.60 g, 2.04 mmol, yield 79%).

4′-Dodecyloxy-4-[pentakis(4-alkoxyphenylethynyl)-phenylethynyl]-biphenyl (6)

Compound **5** was added to a mixture of $K_2(CO)_3$ (930 mg, 6.60 mmol), KI (110 g, 0.66 mmol), 1-bromoalkyl (2.2 mmol) in acetone (20 mL) (700 mg, 0.55 mmol). The mixture was stirred at reflux for 8 h. After cooling, the reaction mixture was filtered. After removal of the solvents, the residue was purified by column chromatography (SiO_2, *n*-hexane–dichloromethane 5 : 1) and crystallized from *n*-hexane to yield **6** as a yellow powder (yield 96–98%).

Spectroscopic data

6a: ^{1}H NMR ($CDCl_3$, 600 MHz): δ 7.64 (d, $J = 7.8$ Hz, 2H), 7.54 (m, 14H), 6.09 (d, $J = 8.4$ Hz, 2H), 6.85 (m, 10H), 4.01 (t, $J = 6.6$ Hz, 2H), 3.97 (m, 10H), 1.80 (m, 12H), 1.49 (m, 12H), 1.35 (m, 20H), 1.00 (t, $J = 7.5$ Hz, 3H), 0.92 (m, 15H). ^{13}C NMR ($CDCl_3$, 150 MHz): δ 159.6, 159.1, 140.9, 133.3, 132.6, 132.2, 128.0, 127.3, 127.2, 126.9, 126.5, 126.5, 121.7, 115.40, 115.37, 114.9, 114.6, 99.3, 99.1, 98.7, 88.4, 86.66, 88.64, 68.1, 67.8, 31.6, 31.4, 29.2, 25.7, 22.6, 19.3, 14.0, 13.9. HRMS (FAB) *m*/*z* for $C_{94}H_{102}O_6$ 1326.7676, found 1326.7686. Anal. calcd for $C_{94}H_{102}O_6$ (1327.8): C 85.03, H 7.74; found: C 84.70, H 8.32.

6b: ^{1}H NMR ($CDCl_3$, 600 MHz): δ 7.64 (d, $J = 7.8$ Hz, 2H), 7.53 (m, 14H), 6.98 (d, $J = 8.4$ Hz, 2H), 6.85 (m, 10H), 4.02 (t, $J = 5.7$ Hz, 2H), 4.01 (m, 10H), 1.79 (m, 12H), 1.48 (m, 12H), 1.36 (m, 24H), 0.93 (m, 18H). ^{13}C NMR ($CDCl_3$, 150 MHz): δ 159.6, 159.1, 140.9, 133.3, 132.6, 132.2, 128.0, 127.3, 127.2, 126.9, 126.6, 126.5, 121.7, 115.5, 115.4, 114.9, 114.6, 99.3, 99.1, 98.7, 88.5, 86.74, 86.70, 68.1, 68.1, 31.6, 31.6, 29.2, 29.2, 25.7, 25.7, 22.6, 22.6, 14.1, 14.1. HRMS (FAB) *m*/*z* for $C_{96}H_{106}O_6$ 1354.7989, found 1354.7997. Anal. calcd for $C_{96}H_{106}O_6$ (1355.9): C 85.04, H 7.88; found: C 85.01, H 7.92.

6c: ^{1}H NMR ($CDCl_3$, 600 MHz): δ 7.62 (d, $J = 8.4$ Hz, 2H), 7.57 (m, 14H), 7.00 (d, $J = 9.0$ Hz, 2H), 6.88 (m, 10H), 4.00 (t, $J = 6.6$ Hz, 2H), 4.00 (m, 10H), 1.82 (m, 12H), 1.49 (m, 12H), 1.36 (m, 28H), 0.94 (m, 18H), 0.92 (t, $J = 7.2$ Hz, 3H). ^{13}C NMR ($CDCl_3$, 150 MHz): δ 159.6, 159.1, 140.9, 133.4, 132.5, 132.2, 128.1, 127.2, 127.1, 126.9, 126.5, 126.5, 121.6, 115.3, 114.8, 114.6, 99.3, 99.2, 98.8, 88.4, 86.6, 68.1, 68.1, 31.9, 31.6, 29.6, 29.4, 29.3, 29.2, 26.1, 25.8, 22.7, 22.7, 14.2, 14.1. HRMS (FAB) *m*/*z* for $C_{98}H_{110}O_6$ 1382.8302, found 1382.8342. Anal. calcd for $C_{98}H_{110}O_6$ (1383.9): C 85.05, H 8.01; found: C 84.82, H 8.03.

6d: ^{1}H NMR ($CDCl_3$, 600 MHz): δ 7.62 (d, $J = 8.4$ Hz, 2H), 7.52 (m, 14H), 6.96 (d, $J = 8.4$ Hz, 2H), 6.83 (m, 10H), 3.98 (t, $J = 6.6$ Hz, 2H), 3.95 (m, 10H), 1.77 (m, 12H), 1.45 (m, 12H), 1.30 (m, 36H), 0.91 (m, $J = 7.5$ Hz, 15H), 0.88 (t, $J = 8.7$ Hz, 3H). ^{13}C NMR ($CDCl_3$, 150 MHz): δ 159.6, 159.1, 140.9, 133.3, 132.6, 132.2, 128.0, 127.3, 127.2, 127.0, 126.6, 126.5, 121.7, 115.5, 114.9, 114.6, 99.3, 99.1, 98.7, 88.5, 86.7, 68.1, 68.1, 32.0, 31.6, 29.7, 29.7, 29.7, 29.5, 29.4, 29.4, 29.3, 29.2, 26.1, 25.7, 22.7, 22.6, 14.1, 14.1. HRMS (FAB) *m*/*z* for $C_{102}H_{118}O_6$ 1438.8928, found 1438.8965. Anal. calcd for $C_{102}H_{118}O_6$ (1440.0): C 85.07, H 8.26; found: C 84.70, H 8.32.

7: ^{1}H NMR ($CDCl_3$, 600 MHz): δ 7.54 (m, 12H), 7.36 (d, $J = 8.4$ Hz, 2H), 6.86 (m, 10H), 6.10 (m, 1H), 3.98 (t, $J = 6.6$ Hz, 10H), 3.63 (m, 1H), 3.52 (m, 2H), 2.59 (m, 2H), 2.47 (m, 1H), 2.24 (m, 1H), 2.09 (m, 1H), 1.80 (m, 11H), 1.60 (m, 4H), 1.47 (m, 10H), 1.33 (m, 24H), 0.91 (m, 18H). ^{13}C NMR ($CDCl_3$, 150 MHz): δ 159.6, 141.8, 135.8, 133.3, 131.7, 127.2, 127.1, 126.9, 126.6, 124.9, 123.0, 121.7, 115.4, 115.3, 114.6, 99.3, 99.1, 98.8, 88.2, 86.7, 86.6, 73.8, 68.4, 68.1, 32.5, 31.8, 31.6, 30.2, 29.2, 28.2, 26.0, 25.8, 25.7, 22.6, 22.6, 14.1, 14.1. HRMS (EI) *m*/*z* for $C_{96}H_{110}O_6$ 1358.8302, found 1358.8358.

8: ^{1}H NMR ($CDCl_3$, 600 MHz): δ 7.64 (d, $J = 8.4$ Hz, 2H), 7.52 (m, 14H), 7.14 (m, 10H), 6.97 (d, $J = 8.4$ Hz, 2H), 4.00 (t, $J = 6.6$ Hz, 2H), 2.62 (m, 10H), 1.81 (m, 4H), 1.62 (m, 10H), 1.47 (m, 2H), 1.30 (m, 64H), 0.88 (m, 18H). ^{13}C NMR ($CDCl_3$, 150 MHz): δ 159.1, 144.0, 143.9, 141.0, 132.6, 132.3, 131.8, 128.53, 128.51, 128.0, 127.43, 127.37, 127.34, 127.2, 126.5, 121.6, 120.6, 114.9, 99.51, 99.45, 99.2, 88.2, 87.2, 68.2, 36.1, 32.0, 31.9, 31.9, 29.7, 29.7, 29.7, 29.6, 29.5, 29.5, 29.4, 29.34, 29.30, 26.1, 22.7, 14.1. HRMS (EI) *m*/*z* for $C_{112}H_{138}O$ 1499.0748, found 1499.0769. Anal. calcd for $C_{112}H_{138}O$ (1500.3): C 89.66, H 9.27; found: C 89.69, H 9.25.

9: ^{1}H NMR ($CDCl_3$, 600 MHz): δ 7.61 (d, $J = 8.4$ Hz, 2H), 7.53 (t, $J = 8.4$ Hz, 2H), 7.50 (m, 12H), 7.29 (d, $J = 7.8$ Hz, 2H), 7.13 (m, 10H), 2.68 (t, $J = 7.8$ Hz, 2H), 2.64 (m, 10H), 1.65 (m, 12H), 1.34 (m, 68H), 0.90 (m, 18H). ^{13}C NMR ($CDCl_3$, 150 MHz): δ 144.17, 144.15, 142.9, 141.2, 137.5, 132.3, 131.8, 129.0, 128.5,

127.4, 127.3, 127.2, 127.1, 126.7, 126.67, 121.9, 120.4, 99.61, 99.56, 99.52, 99.2, 88.3, 87.11, 87.07, 87.05, 36.0, 35.6, 31.9, 31.5, 31.3, 29.72, 29.68, 29.6, 29.39, 29.42, 29.34, 22.7, 13.9. HRMS (EI) *m/z* for $C_{112}H_{138}$ 1483.0799, found 1499.0769. Anal. calcd for $C_{112}H_{138}$ (1484.3): C 90.63, H 9.37; found: C 89.69, H 9.25.

Notes and references

1 K. Kawata, *Chem. Rec.*, 2002, **2**, 59–80.
2 H. Mori, Y. Itoh, Y. Nishiura, T. Nakamura and Y. Shinagawa, *Jpn. J. Appl. Phys.*, 1997, **36**, 143–147.
3 B. Ważyńska and J. A. Okowiak, *Tribol. Lett.*, 2006, **24**, 1–5.
4 H. Zhao, *Chem. Eng. Commun.*, 2006, **193**, 1660–1677.
5 A. N. Cammidge and R. J. Bushby, in *Handbook of Liquid Crystals*, ed. D. Demus, J. Goodby, G. W. Gray and H.-W. Spiess, Wiley-VCH, Weinheim, Germany, 1998, vol. 2B.
6 S. Chandrasekhar, in *Handbook of Liquid Crystals*, ed. D. Demus, J. Goodby, G. W. Gray and H.-W. Spiess, Wiley-VCH, Weinheim, Germany, 1998, vol. 2B.
7 M. Ebert, D. A. Jungbauer, R. Kleppinger, J. H. Wendorff, B. Kohne and K. Praefcke, *Liq. Cryst.*, 1989, **4**, 53–67.
8 B. Kohne and K. Praefcke, *Chimia*, 1987, **41**, 196–198.
9 S. Marguet, D. Markovitsi, D. Goldmann, D. Janietz, K. Praefcke and D. Singer, *J. Chem. Soc., Faraday Trans.*, 1997, **93**, 147–155.
10 K. Praecfcke, D. Singer, B. Gundogan, K. Gutbier and M. Langner, *Ber. Bunsenges. Phys. Chem.*, 1993, **97**, 1358–1361.
11 K. Praefcke, B. Kohne, K. Gutbier, N. Johnen and D. Singer, *Liq. Cryst.*, 1989, **5**, 233–249.
12 K. Praefcke, B. Kohne and D. Singer, *Angew. Chem., Int. Ed. Engl.*, 1990, **29**, 177–179.
13 S. Kumar and S. K. Varshney, *Angew. Chem., Int. Ed.*, 2000, **39**, 3140–3142.
14 S. Kumar, S. K. Varshney and D. Chauhan, *Mol. Cryst. Liq. Cryst.*, 2003, **396**, 241–250.
15 S. Kohmoto, E. Mori and K. Kishikawa, *J. Am. Chem. Soc.*, 2007, **129**, 13364–13365.
16 M. W. Day, A. J. Matzger and R. H. Grubbs, Private communication to CCDC, 2001, ref. code OCUKOM.
17 S.-C. Chien, H.-H. Chen, H.-C. Chen, Y.-L. Yang, H.-F. Hsu, T.-L. Shih and J.-J. Lee, *Adv. Funct. Mater.*, 2007, **17**, 1896–1902.
18 P. H. J. Kouwer and G. H. Mehl, *J. Mater. Chem.*, 2009, **19**, 1564–1575.
19 S. K. Varshney, V. Prasad and H. Takezoe, *Liq. Cryst.*, 2011, **38**, 53–60.
20 H. K. Bisoyi and S. Kumar, *Chem. Soc. Rev.*, 2010, **39**, 264–285.
21 C. Tschierske and D. J. Photinos, *J. Mater. Chem.*, 2010, **20**, 4263–4294.
22 C. Keith, A. Lehmann, U. Baumeister, M. Prehmab and C. Tschierske, *Soft Matter*, 2010, **6**, 1704–1721.

